Lawrence Berkeley Laboratory
UNIVERSITY OF CALIFORNIA

Accelerator & Fusion Research Division
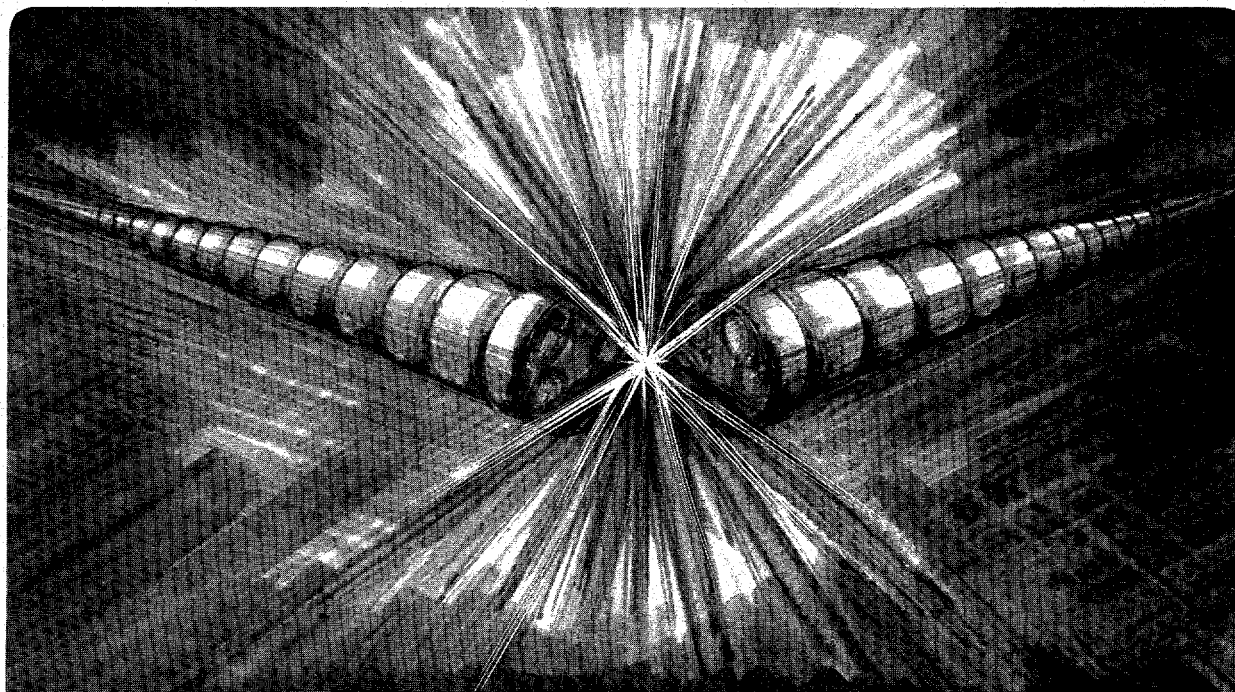
RECEIVED

FEB 15 1996

OSTI

Ultra-High Resolution Spectroscopy of the He Doubly Excited States

J.D. Bozek, A.S. Schlachter, G. Kaindl, and K. Schulz

November 1995

DISCLAIMER

DISCLAIMER

Portions of this document may be illegible in electronic image products. Images are produced from the best available original document.

ULTRA-HIGH RESOLUTION SPECTROSCOPY
OF THE HE DOUBLY EXCITED STATES*

J.D. Bozek and A.S. Schlachter
Advanced Light Source
Accelerator and Fusion Research Division
Lawrence Berkeley National Laboratory
Berkeley, CA 94720, USA

G. Kaindl and K. Schulz
Institut für Experimentalphysik
Freie Universität Berlin
Arnimalle 14, D-14195 Berlin-Dahlem
Germany

ULTRA-HIGH RESOLUTION SPECTROSCOPY OF THE HE DOUBLY EXCITED STATES

J.D. BOZEK, P.A. HEIMANN AND A.S. SCHLACHTER
Advanced Light Source, Lawrence Berkeley National Laboratory, Mail Stop 2-400, 1 Cyclotron Road, Berkeley, California 94720, U.S.A.

and

G. KAINDL AND K. SCHULZ
Institut für Experimentalphysik, Freie Universität Berlin, Arnimalle 14, D-14195 Berlin-Dahlem, Germany

Abstract

Photoionization spectra of the doubly-excited states of He were measured using beamline 9.0.1 at the Advanced Light Source. The beamline utilizes a 4.5 m long 8 cm period undulator as its source together with a spherical grating monochromator to provide an extremely bright source of photons in the range of 20 - 300 eV. A resolving power ($E/\Delta E$) of 64,000 was obtained from the 1 meV FWHM (2p,3d) doubly excited state resonance of He at 64.12 eV. The high brightness of the source and the very high quality optical elements of the beamline were all essential for achieving such a high resolution. The beamline components and operation are described and spectra of the double excitation resonances of He presented.

1. Introduction

Helium is a favorite target of physicists interested in studying electron-electron correlation owing to it being the simplest two electron system. Additionally, this simplicity permits calculations of the highest complexity to be carried out and compared with the experimental results. Double excitation was first recognized in photoabsorption spectra of He by Madden and Codling [1] and explained by Cooper, Fano and Prats [2] over 30 years ago. Consistent

improvements in photon resolution and flux have facilitated the identification of an ever increasing number of series of doubly-excited states in He. Most recently, Kaindl and coworkers have published an extensive survey of the double excitation spectra of He [3] using the highest available photon resolution, 4 meV. They identified resonances belonging to 18 different Rydberg series below the $N = 2$ to $N = 9$ ionization thresholds of He and reported energies, widths, Fano-q parameters and quantum defects for the various resonances and series. With the introduction of one of the first third generation synchrotrons, the Advanced Light Source (ALS) [4], and commissioning of a new high resolution beamline for atomic and molecular physics, beamline 9.0.1 [5], it is not surprising that the double excitation spectra of He have been revisited.

Double excitation resonances appear in the single ionization continuum of He resulting from the simultaneous excitation of both electrons, an "inner" one into the $N \geq 2$ shell and an "outer" one into the $n \geq N$ shell. These autoionizing resonances occur as series of Rydberg levels over the photon energy range of 60 to 79 eV, corresponding to the excitation of both electrons into the $N = 2$ level at the lower energy extent and the double ionization threshold at the higher energy. The first double excitation Rydberg series, with the inner electron in the $N = 2$ shell and the outer electron in the $n = 2, 3, 4, \ldots$ shells covers the range from 60 eV, where the $(N = 2, n = 2)$ states is observed, up to 65.4 eV, the $N = 2$ ionization threshold of He, IP_2, corresponding to the first excited state $(N = 2)$ of He^+.

Two common classification schemes are used to describe the electronic configuration of doubly excited He. The principle quantum numbers N of the inner electron and n of the outer electron are used to describe the doubly excited state. For each inner electron quantum level, N, $(2N-1)$ Rydberg series of $^1P^0$ final states are dipole allowed for photon absorption. The first set of series, where $N = 2$, can be adequately described using the scheme introduced by Madden and Codling [1] where the three allowed series are denoted (sp,2n+), (sp,2n-) and (2p,nd). This scheme is similar to the simple MO model where the (sp,2n+) and (sp,2n-) doubly-excited orbitals are composed of coherent and incoherent superpositions of the (2p,ns) and (2s,np) wave functions. Beyond the second ionization threshold, however, the increasing number of allowed states makes this type of scheme unwieldy. A classification based on the hyperspherical coordinate description of He was introduced (see [6]) and doubly excited states are denoted by N,K_n in the short hand form where N and n have their usual meanings and K ranges from $N-1-T$ to -$(N-1-T)$ with $T = 0$ or 1. In this scheme, the (sp,2n+), (sp,2n-) and (2p,nd) series are written as $2,0_n$, $2,1_n$ and $2,-1_n$ respectively. The older scheme will be used to discuss the resonances shown here as only those occurring below IP_2 will be considered.

2. Methods

Beamline 9.0.1 at the Advanced Light Source was designed, constructed and commissioned by a team of scientists and engineers led by P.A. Heimann and R. DiGennaro of Lawrence Berkeley National Laboratory [5]. Their careful work resulted in a beamline which has met and in some ways surpassed its design goal of providing 10^{12} photons per second with a resolving power (E/ΔE) of 10,000 over the full useable range of the spherical grating monochromator (SGM), 20 - 300 eV. Flexibility in the optical configuration of the beamline permits a wide range of trade-offs between flux and spectral resolution.
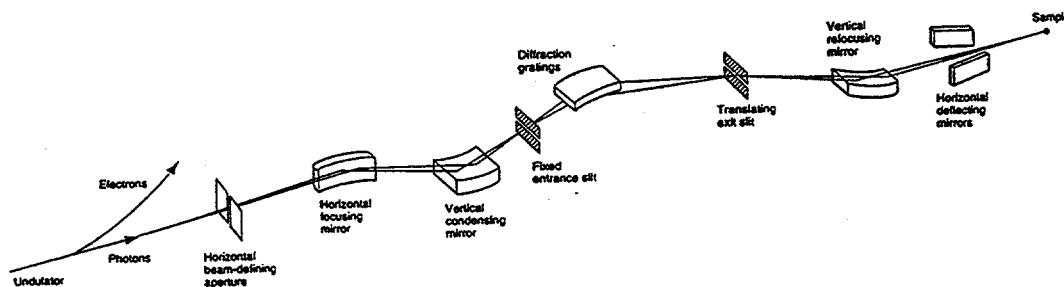

Figure 1. Schematic diagram of beamline 9.0.1 showing the major components.

A schematic diagram of the important elements of this SGM beamline is given in Figure 1. A 4.5 m long 8 cm period undulator in the low-emittance ALS storage ring served as the source for the beamline. The importance of high brightness for high spectral resolution cannot be overemphasized; because of the high brightness (low-emittance) photons are emitted from the undulator in a very narrow central cone. An adjustable horizontal aperture between the undulator and the first optical element of the beamline scrapes away unwanted off-axis radiation reducing the heat load for the more sensitive optical surfaces. A horizontal spherical mirror focuses the radiation to form a 1:1 horizontal image of the source at the sample location. The spherical vertical condensing mirror demagnifies the source 8:1 onto the entrance slit. The small divergence of the beam from the undulator together with the high quality of the optical surfaces permits most of the photon beam to be passed through a 10 μm entrance slit, preserving the high intensity of the source. The water cooled entrance slit is variable from 100 μm to fully closed. One

of three spherical diffraction gratings with 380, 925 and 2100 lines/mm can be selected to disperse the radiation. All of the optics up to and including the diffraction grating are made from Glidcop, a special copper alloy, and actively cooled by a closed loop water circulation system kept at $20.0 \pm 0.1°C$. The exit slit translates along a granite slab on the optical axis of the monochromator in order to satisfy the focusing condition of the SGM. A variable radius refocusing mirror forms an image of the exit slit at the sample position. The spot size at the sample is less than 1 mm FWHM in both the horizontal and vertical directions.
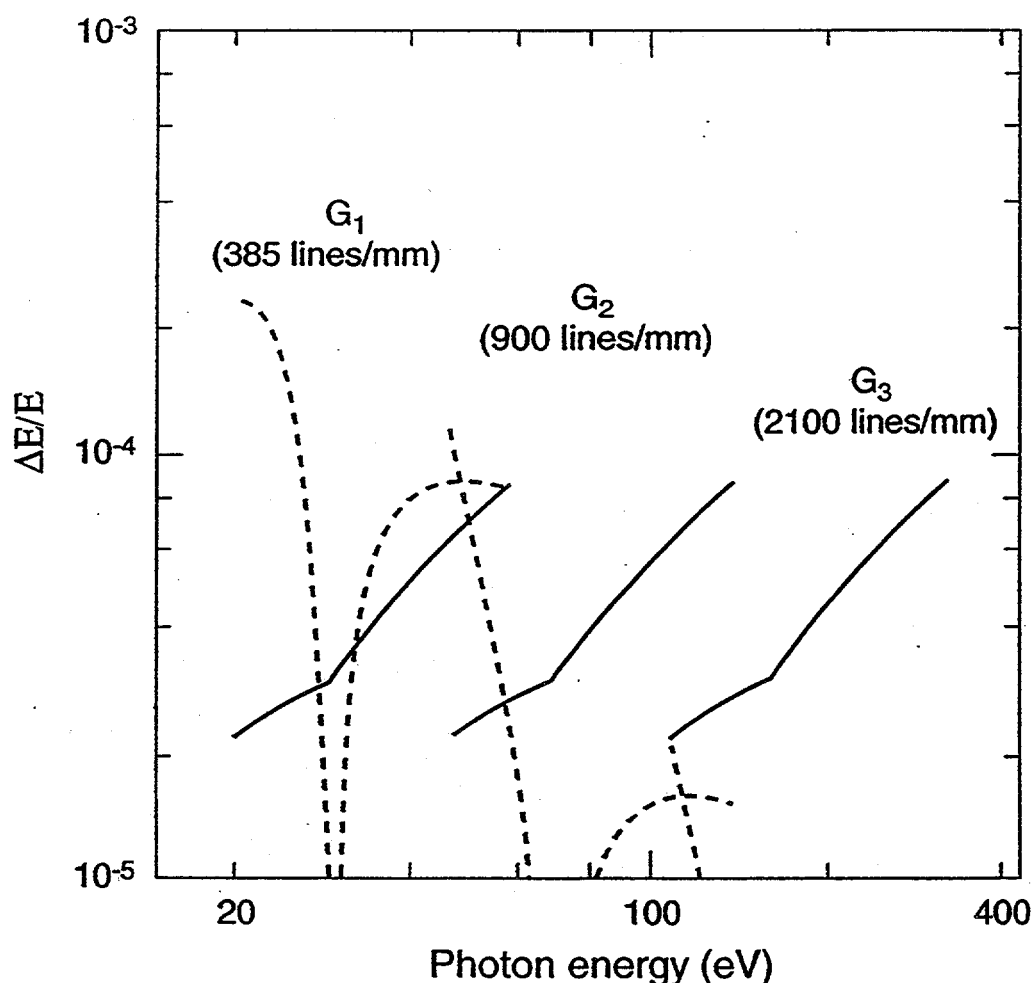

Figure 2. Resolution of the SGM as function of photon energy. The solid lines show the resolution contribution of 10 μm slits. The dashed lines show the contributions of spherical coma.

The ultimate resolution of the beamline is determined by the finite width of the slits and contributions from the aberration coma, of the grating. Figure 2 shows the limits of the resolution from both factors as a function of photon energy for all three gratings. The double excitation resonances of He fortuitously lie in a region

where the coma for the second grating drops towards zero at the Rowland circle geometry. The resolution is therefore limited primarily by the width of the slits. At small slit widths, however, other usually less significant contributions to the resolution become important, such as the figure of the optical surfaces. The grating surface, for example, was ordered from Rocketdyne with a specified slope error tolerance of ≤ 0.5 µrad rms. This slope error will add some small contribution to the bandwidth of the beamline.

Photoionization spectra of He were measured using a gas cell attached to the end of the beamline. The gas cell consisted of two 10 cm long parallel charge collecting plates centered along the photon beam and separated from the vacuum of the beamline by a thin Al or C window. The cell was charged with between 1 and 300 milliTorr of He, one plate biased with 100 V and the ion current measured on the second plate. The incident photon flux was monitored simultaneously by measuring the current on a 90% transmitting gold grid inserted into the incident beam. Currents from both the plate and the grid were converted to voltages using
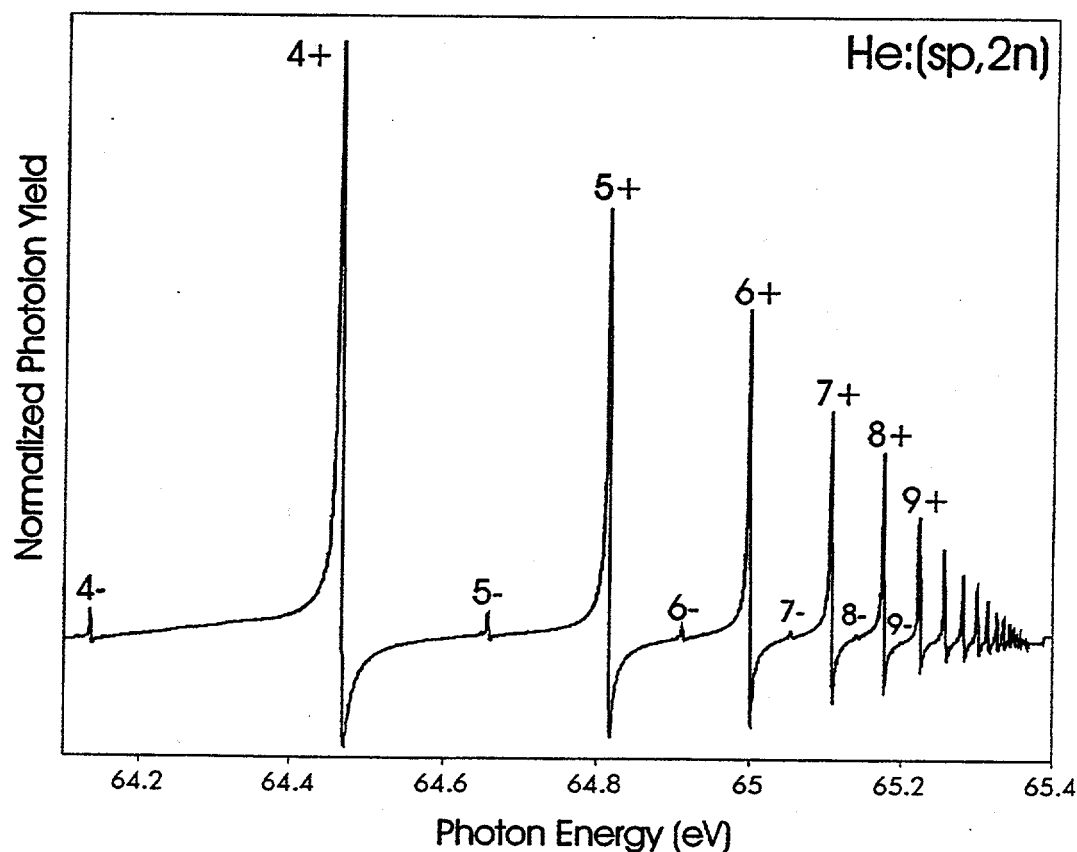

Figure 3: A wide range scan of the doubly excited states of He below the second ionization potential, IP_2. Numbers, n, on the figure denote the assignment of the peaks as either (sp,2n+) or (sp,2n-).

two Keithley 428 current amplifiers and integrated for the desired period by counting pulses from voltage to frequency converters. All spectra reported here have been normalized for the incident photon flux variations by dividing the ion current signal by the gold mesh current signal.

3. Results

A wide range scan of the double excitation resonances of He below the second ionization potential, IP_2, is shown in Figure 3. This spectrum was recorded with 6 μm entrance and exit slits, 2 seconds per point and 0.6 meV step size. Peaks from the three optically allowed Rydberg series converging to the ionization limit can be clearly seen in this wide range scan. Using the notation first adopted by Madden and Codling [1], the series of intense peaks correspond to the (sp,2n+) series, the weaker intervening resonances to the (sp,2n-) series. The very much weaker (2p,nd) resonances can barely be seen just below the "-" resonances but are not labeled on this figure. The (sp,2/2+), (sp,2/3+) and (sp,2/3-) resonances are not seen in Fig. 3 as they occur at lower photon energies.

The region close to threshold is not clearly seen in Fig. 3 and has been expanded in Figure 4. Resonances up to (sp,2/26+) are seen in this data set, representing a substantial improvement over the best previous results [3]. The number of (n+) resonances resolved is directly related to the resolution since the
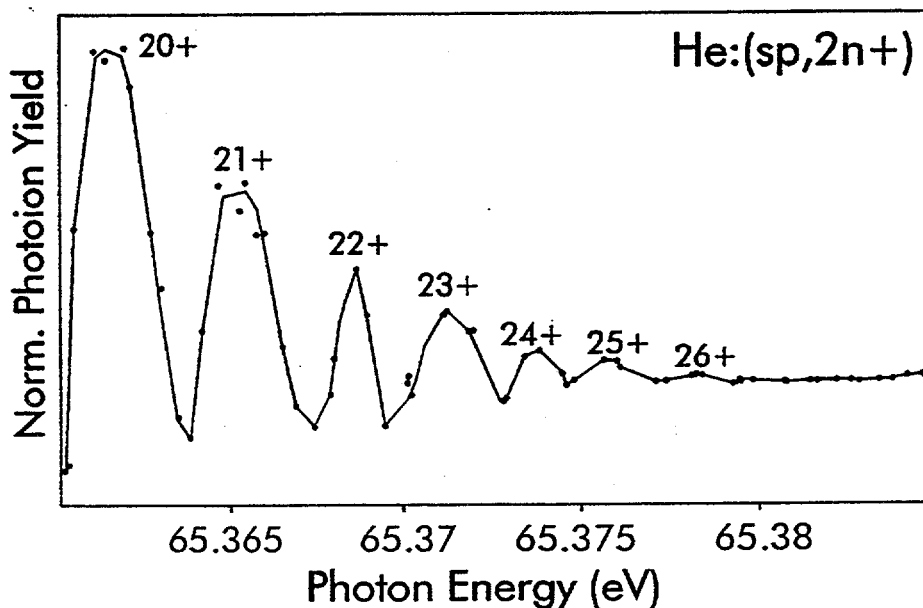

Figure 4: Expanded view of the (sp,2n+) doubly excited resonances of He close to the ionization threshold.

natural widths of these states scale with the inverse of the effective quantum number cubed [7].

Closer views around the (n-) and (2p,nd) resonances are presented in Figure 5. These spectra were measured with narrower slits and smaller energy step sizes than the wide range scan. The high resolution of the SGM, made possible by the high brightness source preserving significant flux through the small entrance slit, clearly resolves the (2p,nd) resonances from the neighboring (n-) peaks and will permit a more accurate determination of the energy and line shape parameters for these lines. A further increase in scale for the (2p,3d) state, separated from the neighboring 4- state by only 17 meV is given in Figure 6. This spectrum was measured with 2.5 μm entrance and exit slits and a FWHM of 1.0 meV was obtained. The natural width of the (2p,3d) resonance has been calculated to be less than 3 μeV [3]. The 1.0 meV experimental resolution corresponds to an experimental resolving power of 64,000 at a photon energy of 64.1 eV ! This resolution represents a factor of four increase over the previous best resolution in this photon energy range [3].
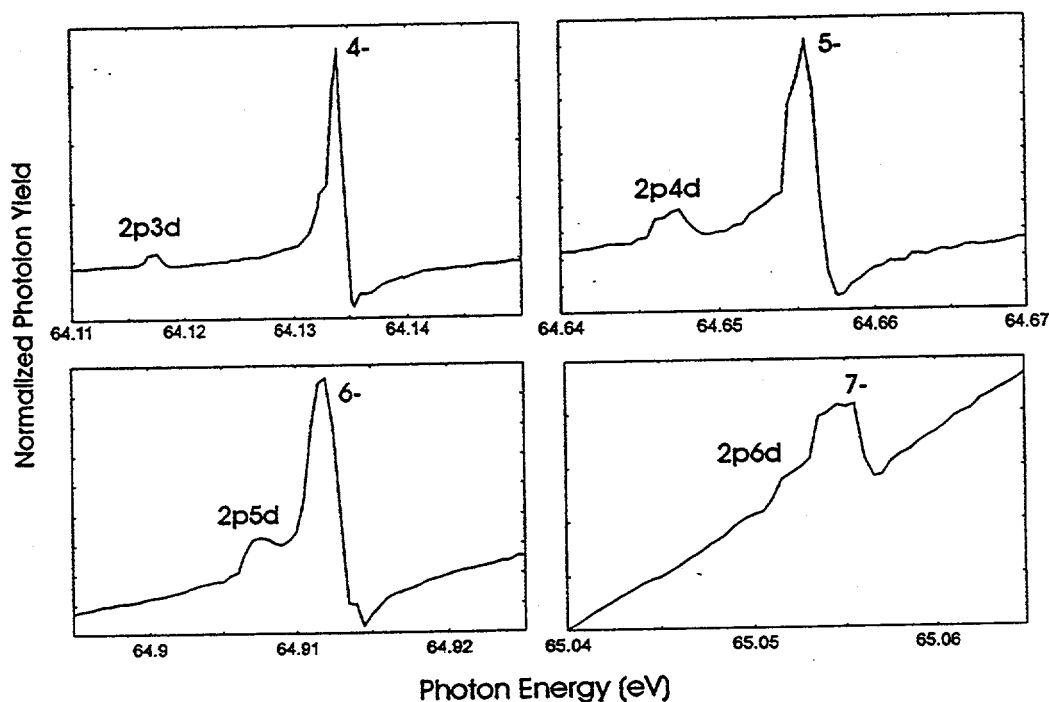

Figure 5: Expanded views of the (4-), (5-), (6-) and (7-) resonances and neighboring (2p,nd) resonances.

The drive motor for the monochromator was slowed and the energy steps reduced to 0.4 meV for the (2p,3d) spectrum in Fig. 6. Several other optimizations of the beamline were required to achieve the highest resolution. The vertical focusing mirror (M2) was found to be particularly sensitive to vibrations induced by turbulent water flow through the cooling channels. By reducing the flow of water, variations in the incident intensity were dramatically reduced. Intensity variations of about 0.5% remained in the incident beam following attempts to minimize all sources of mechanical motion in the optics.

The unprecedented resolving power of 64,000 in this energy range is a testament to the careful design and fabrication of this beamline and its optics. The ultimate resolution of the 18 cm long 925 line/mm grating is 0.4 meV, determined by the number of lines on the optical surface, 166,500. Contributions from slope errors on the grating surface are calculated to be about 1.1 meV at 64 eV using the specification value. Since the 2.5 μm slits contribute about 0.5 meV, the grating figure must be better than the 0.5 μrad in the specification.
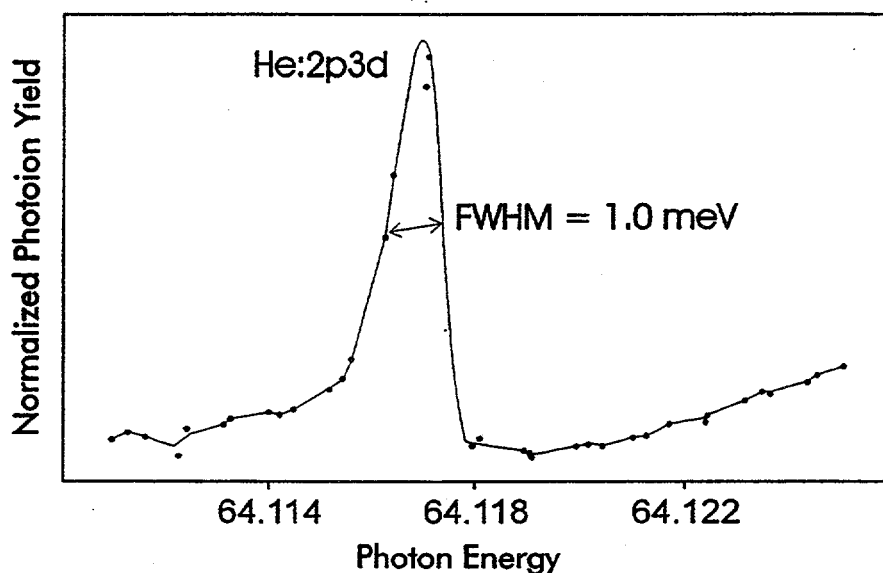

Figure 6: Expansion of the (2p,3d) resonance with a FWHM of 1.0 meV.

All of the optically accessible double excitation series of He were studied and the results will be presented elsewhere together with least squares fits to the data [8]. Further improvements in the experimental data are expected both in the resolution of the SGM and in the signal to noise level of the data, especially close to

threshold where the resonances are very weak, in the near future using the existing equipment with upgraded electronics.

4. Acknowledgments

5. References

1. R.P Madden and K. Codling, Phys. Rev. Lett., 10 (1963) 516; Astrophys. J., 141 (1965) 364.
2. J.W. Cooper, U. Fano and F. Prats, Phys. Rev. Lett. 10 (1963) 518.
3. M. Domke, K. Schulz, G. Remmers, G. Kaindl and D. Wintgen, Phys. Rev. A, submitted (1995).
4. A.L. Robinson and A.S. Schlachter, Nucl. Instrum. and Methods A319 (1992) 40.
5. P.A. Heimann, D. Mossessian and J.D. Bozek, Advanced Light Source Project Document LSBL-239, Lawrence Berkeley National Laboratory, Berkeley, CA (1994).
6. M. Zubek, G.C. King, P.M. Rutter and F.H Read, J. Phys. B, 22 (1989) 3411.
7. K. Schulz, G. Kaindl, J.D. Bozek, P.A. Heimann and A.S. Schlachter, J. Electron Spectrosc. Relat. Phenom., submitted (1995).
8. K. Schulz, G. Kaindl, J.D. Bozek, P.A. Heimann and A.S. Schlachter, to be published.